

Special Section on 50 Years of Opioid Research

Unique Pharmacological Properties of the Kappa Opioid Receptor Signaling Through $G_{\alpha z}$ as Shown with Bioluminescence Resonance Energy Transfer

Miriam E. Barnett, Brian I. Knapp, and  Jean M. Bidlack

Department of Pharmacology and Physiology, University of Rochester, School of Medicine and Dentistry, Rochester, New York

Received January 6, 2020; accepted July 16, 2020

ABSTRACT

Opioid receptors (ORs) convert extracellular messages to signaling events by coupling to the heterotrimeric G proteins, $G_{\alpha\beta\gamma}$. Classic pharmacological methods, such as [^{35}S]GTP γS binding and inhibition of cyclic AMP production, allow for general opioid characterization, but they are subject to the varying endogenous G_{α} proteins in a given cell type. Bioluminescence resonance energy transfer (BRET) technology offers new insight by allowing the direct observation of G_{α} subunit-specific effects on opioid pharmacology. Using a Venus-tagged $G_{\beta\gamma}$ and nanoluciferase-tagged truncated G protein receptor kinase 3, an increase in BRET signal correlated with OR activation mediated by a specific G_{α} protein. The magnitude of the BRET signal was normalized to the maximum response obtained with 10 μM 2-(3,4-dichlorophenyl)-*N*-methyl-*N*-[(1*R*,2*R*)-2-pyrrolidin-1-ylcyclohexyl]acetamide (U50,488) for the kappa OR (KOR). Opioids reached equilibrium with the KOR, and concentration-response curves were generated. Although the full agonists U50,488, salvinorin A, nalurfafine, and dynorphin peptides were equally efficacious regardless of the G_{α} subunit present, the concentration-response curves were leftward shifted when the KOR was signaling through $G_{\alpha z}$ compared with other $G_{\alpha i/o}$

subunits. In contrast, the G_{α} subunit distinctly affected both the efficacy and potency of partial kappa agonists, such as the benzomorphans, and the classic mu opioid antagonists, naloxone, naltrexone, and nalmefene. For example, (-)pentazocine had EC_{50} values of 7.3 and 110 nM and maximal stimulation values of 79% and 35% when the KOR signaled through $G_{\alpha z}$ and $G_{\alpha i1}$, respectively. Together, these observations suggest KOR pharmacology varies based on the specific G_{α} subunit coupled to the KOR.

SIGNIFICANCE STATEMENT

Opioid receptors couple to various heterotrimeric $G_{\alpha\beta\gamma}$ proteins to convert extracellular cues to precise intracellular events. This paper focuses on how the various inhibitory G_{α} subunits influence the pharmacology of full and partial agonists at the kappa opioid receptor. Using a bioluminescent assay, the efficacy and potency of kappa opioids was determined. Opioid signaling was more potent through $G_{\alpha z}$ compared with other G_{α} proteins. These observations suggest that $G_{\alpha z}$ may impact opioid pharmacology and cellular physiology more than previously thought.

Introduction

Kappa opioid receptors (KORs), members of the classic seven-transmembrane G protein-coupled receptor (GPCR) family, transduce extracellular cues into intracellular signaling events through receptor-coupled heterotrimeric G proteins,

This work was supported by National Institutes of Health National Institute of General Medical Sciences [Grant GM068411] (M.E.B.) and the National Institute on Drug Abuse [Grant DA046817] (J.M.B.). The J.R. Murlin Memorial Fund (M.E.B.) and the Margo Cleveland Fund (J.M.B.) also supported this research.

<https://doi.org/10.1124/mol.120.119404>.

$G_{\alpha\beta\gamma}$. When stimulated by an opioid, activated opioid receptors (ORs) initiate a conformational change in the G_{α} subunit (Rasmussen et al., 2011). This change allows for the binding of GTP to the G_{α} subunit, which in turn allows the activated G_{α} to dissociate from $G_{\beta\gamma}$ and the OR (Kenakin, 2011). G_{α} and $G_{\beta\gamma}$ can then independently associate with their downstream effectors. For example, G_{α} proteins interact with adenylyl cyclase (AC) to regulate intracellular cAMP concentrations. The signal is terminated when the GTP bound to the G_{α} subunit is hydrolyzed to GDP and G_{α} again associates with $G_{\beta\gamma}$ and the OR.

ABBREVIATIONS: AC, adenylyl cyclase; BRET, bioluminescence resonance energy transfer; E_{max} , maximal stimulation; fwd, forward; GAPDH, glyceraldehyde-3-phosphate dehydrogenase; GPCR, G protein-coupled receptor; GRK3, G protein-coupled receptor kinase 3; GRK3ct, G protein-coupled receptor kinase 3 C terminus; HEK, human embryonic kidney; KOR, kappa opioid receptor; mas, myristic acid attachment peptide (MGSSKSKSTSNS); MOR, mu opioid receptor; Mr 2033, ((±)- α -5,9-dimethyl-2-(*L*-tetrahydrofurfuryl)-2'-hydroxy-6,7-benzomorphan) hydrochloride; nLuc, nanoluciferase; nor-BNI, norbinaltorphimine; OR, opioid receptor; rev, reverse; RGS, regulator of G protein signaling; U50,488, 2-(3,4-dichlorophenyl)-*N*-methyl-*N*-[(1*R*,2*R*)-2-pyrrolidin-1-ylcyclohexyl]acetamide.

There are four families of Gα proteins (Gαi, Gαs, Gαq, Gα13) that share features including a guanine nucleotide binding site, intrinsic GTPase activity, and lipid modifiers to facilitate localization to the plasma membrane (Wedegaertner et al., 1995; Syrovatkina et al., 2016; Hilger et al., 2018). Differences between the families are based on sequence homology, distinct downstream effectors, and toxin sensitivity (Glick et al., 1998; Milligan and Kostenis, 2006). KORs predominately couple to the Gαi class, comprising Gαi1, Gαi2, Gαi3, GαoA, GαoB, and Gαz. Since all members of this class inhibit AC activity and thus decrease cAMP levels, it is common to downplay the differences that exist within this Gα class. However, when individual Gα subunits within the inhibitory Gα class were knocked down by intracerebroventricular administration of Gα siRNA into the right ventricle of mice, differences in the activation profiles of various OR agonists were observed (Sánchez-Blázquez et al., 1999, 2001). Thus, the growing evidence that the unique GPCR•Gα interaction could influence signaling creates a much more complex picture than previously thought.

Current in vitro pharmacological methods, however, lack the specificity needed to distinguish contributions from unique Gα-mediated signaling. For example, it is common to correlate changes in cAMP levels to OR activation. This assay has several limitations. First, changes in cAMP are subject to amplification from many converging pathways including signaling from competing Gαs proteins (Yung et al., 1995). Additionally, cell lines may express up to nine isoforms of AC, to which the Gα proteins couple to varying degrees (Sadana and Dessauer, 2009). Thus, by simply measuring changes in cAMP levels in a given cell line, we are looking downstream of the OR and not accounting for the specific Gα protein. In contrast, the [³⁵S]GTPγS binding assay measures the binding of nonhydrolyzable GTPγS to the Gα subunit, the initial step in GPCR signaling, and thus is not subject to influences from concurrent signaling pathways. However, this assay still fails to account for the specific Gα subunit coupled to the receptor or the pool of available Gα subunits in a given cell line (Traynor and Nahorski, 1995; Bidlack and Parkhill, 2004). Although these aforementioned assays have offered insight into the OR signaling mechanisms and opioid pharmacology, determining how the cellular environment of G proteins influences OR signaling will be useful in obtaining a more thorough understanding of opioid receptor signaling.

To address the limitations of prior methods, researchers have adapted a novel bioluminescence resonance energy transfer (BRET)-based assay. BRET monitors protein-protein interactions in live cells with the necessary sensitivity to view G protein signaling (Stoddart et al., 2015). Previous data from our laboratory using BRET to obtain the Gα-specific pharmacological profiles of buprenorphine and samidorphan showed that the KOR signaling was very sensitive to the Gα subunit (Bidlack et al., 2018). For instance, at the KOR, the 1:3 molar combination of buprenorphine:samidorphan generated maximal stimulation (E_{max}) values ranging from 22% signaling through Gαi2 to 85% when signaling through Gαz. In this study, we expanded upon this concept and determined how the different Gα subunits from the Gαi/o family influenced the pharmacology of full and partial agonists at the KOR.

Materials and Methods

Cell Culture, Plasmids, and Transfection. Human embryonic kidney (HEK) 293T cells (ATCC, Manassas, VA) were cultured on

poly-L-lysine (Millipore Sigma, Darmstadt, Germany)-coated 100-mm dishes in Dulbecco's modified Eagle's medium (GIBCO, Grand Island, NY) supplemented with 10% fetal bovine serum, 1% nonessential amino acids, 1 mM sodium pyruvate, and 100 U/ml penicillin and streptomycin. Cells were maintained at 37°C in a 5% CO₂ atmosphere. Prior to transfection, 4 × 10⁶ cells were seeded onto a Matrigel-coated (Corning, Inc., Corning, NY) 60-mm dish in antibiotic-free medium and incubated for 4 hours at 37°C and 5% CO₂, as previously described (Masuho et al., 2015a). The human KOR (cDNA Resource Center, Bloomsburg, PA), human Gα subunit of interest (cDNA Resource Center), Venus 156–239-Gβ1, Venus 1–155-Gγ2, or Venus 1–155-Gγ7, and myristic acid attachment peptide (mas) with the C terminus of G protein-coupled receptor kinase (GRK3ct) fused with nanoluciferase (nLuc) plasmids (masGRK3ct-nLuc; gifts from Dr. Kirill A. Martemyanov, The Scripps Research Institute Florida, Jupiter, FL) were transfected at a 1:2:1:1:1 ratio (ratio 1 = 0.42 μg of plasmid DNA) as previously described (Masuho et al., 2015a) using Lipofectamine LTX with PLUS reagent (Invitrogen, Carlsbad, CA) (Masuho et al., 2015a) in antibiotic-free Opti-MEM I Reduced Serum Media (GIBCO).

Measuring KOR Signaling Through Different Gα Subunits Using BRET. BRET measurements between Venus-Gβ1γ2 or Venus-Gβ1γ7 and masGRK3ct-nLuc were performed to determine agonist-dependent activation of the Gα protein of interest in live HEK 293T cells. For each experiment performed, a separate transfection with Gα, Venus-Gβ1γ2, and masGRK3ct-nLuc was also performed to ensure the opioid of interest was not having an effect without the KOR expressed. Additionally, another transfection with the KOR, Venus-Gβ1γ2, and masGRK3ct-nLuc was performed to confirm that endogenous Gα proteins were not contributing to the BRET signal. Cells were prepared 16–20 hours posttransfection as previously described (Masuho et al., 2015a). BRET assays were performed at 25°C in 96-well flat bottom white plates (Greiner Bio-One North America, Inc., Monroe, NC) in a final volume of 100 μl/well. Approximately 75,000 transfected cells per well (25 μl) were incubated for 50 minutes or for varying times with or without opioids in BRET buffer [PBS (GIBCO) with 0.5 mM MgCl₂ and 0.1% glucose]. Plates were read after addition of 25 μl 2× Nano-Glo™ Luciferase Assay Substrate (Promega, Madison, WI) on a Flexstation 3 (Molecular Devices, San Jose, CA) at 535 and 475 nm. The BRET signal was calculated as emission of Venus at 535 nm divided by the emission of nLuc at 475 nm. Each assay was performed in duplicate and repeated with separate transfections at least three times. A baseline, with no opioid stimulation, was set as the minimum BRET value, and 10 μM 2-(3,4-dichlorophenyl)-N-methyl-N-[(1*R*,2*R*)-2-pyrrolidin-1-ylcyclohexyl]acetamide (U50,488), a full KOR agonist, was set as the maximal BRET signal. The mean baseline BRET ratio was subtracted from each experimental BRET ratio to obtain a ΔBRET ratio. All ΔBRET ratios were normalized to the 10 μM U50,488 ΔBRET ratio, which was set at 100%.

Data Analysis and Statistics. Concentration-response curves were generated in SigmaPlot (version 11; Systat Software Inc., San Jose, CA), and E_{max} and EC₅₀ values were calculated from a logistic-3 parameter curve fit of a log-probit plot. Data are expressed as the mean EC₅₀ and E_{max} values ± S.D. from three or more independent experiments, performed in duplicate. The averages of the duplicates for each experiment were used to calculate the mean and S.D. values. The S.D. was computed from the $n \geq 3$ independent experiments. Statistical significance between all Gα subunits was determined using one-way ANOVA with Holm-Sidak post hoc testing. Statistical significance between Gαi1 and Gαz EC₅₀ and E_{max} values were determined using a two-tailed Student's *t* test. All statistical analysis was performed in PRISM software (version 6.0; GraphPad Software Inc., La Jolla, CA).

Western Blotting. Approximately 5 × 10⁶ HEK 293T cells transfected with KOR, Gα subunit of interest, Venus-Gβ1γ2, and masGRK3ct-nLuc were scraped with PBS, containing Roche cOmplete, EDTA-free protease inhibitors (Roche, Indianapolis, IN). Cells were then lysed using a Dounce homogenizer (Dounce et al., 1955;

DeCaprio and Kohl, 2019). Lysates were centrifuged at 18,000g for 20 minutes at 4°C. The soluble fraction was removed. Membrane proteins were extracted by resuspending the pellet in PBS containing EDTA-free protease inhibitors and 0.1% Triton-X 100, with gentle rocking at 4°C for 20 minutes. Samples were centrifuged again at 18,000g for 15 minutes at 4°C. The supernatant was collected, and protein content was determined using Pierce BCA assay kit according to manufacturer's guidelines (Thermo Fisher Scientific, Rochester, NY). Total protein, 50 µg, in 2× Laemmli sample buffer (0.005% bromophenol blue, 4% SDS, 20% glycerol, 120 mM Tris-Cl, pH 6.8) with 5% β-mercaptoethanol (Karlsson et al., 1994) was heated at 100°C for 10 minutes. Samples were separated on a 4%–20% gradient polyacrylamide gel and transferred to a nitrocellulose membrane. Blots were blocked with 5% nonfat dry milk in Tris-buffered saline containing 0.1% Tween 20, pH 7.4, for 60 minutes at room temperature and incubated overnight at 4°C with 1:1000 dilution of polyclonal rabbit anti-human Gα antibody against each Gα subunit (Cell Signaling Technologies, Danvers, MA). Blots were washed for 5 minutes three times with Tris-buffered saline containing 0.1% Tween 20, pH 7.4, and incubated for 60 minutes with a 1:1000 dilution of goat anti-rabbit horseradish peroxidase secondary antibody (Cell Signaling Technologies). A BioRad ChemiDoc chemiluminescent imager (Hercules, CA) was used to image the protein.

Real-Time Quantitative Polymerase Chain Reaction Analysis. Total RNA was extracted from either HEK 293A or CHO cells using E.N.Z.A. Total RNA kit following the manufacturer's protocol (Omega bio-tek, Norcross, GA). cDNA was produced using ThermoScript RT-PCR Systems (Invitrogen). iTaq Universal SYBR Green (Bio-Rad) was used as a double strand DNA-specific dye. Species-specific primers were designed for each Gα subunit in both cell lines. The CHO cell line primers were as follows: *Gai1* [forward (fwd): GGA GGTGAAGATAGACTTTGGAG, reverse (rev): TGCAGAATCATTGA GCTGGTACTC], *Gai2* (fwd: CTGAGGAACAAGGGATGCTGC, rev: GTTTTCACACGGGTCCGCA), *Gai3* (fwd: AGGCGTGATTAACG GCTCT, rev: AGTGTGTCTCCACAATGCCT), *GαO* (fwd: GCCAAA GACGTGAAATTACTCC, rev: AGTATCCATGGCCCGGACGATGGC), and *Gαz* (fwd: AAGCTCTATGAGGATAACCAGACG, rev: TACGTG TTCTGACCCTTGACTCT). The HEK 293 cell line primers were as follows: *Gai1* (fwd: GGAGTTGAAGATAGACTTTGGTG, rev: TGC AGAATCATTAAAGCTGGTACTC), *Gai2* (fwd: ACAACATCCTCAAGG GCTCAAG, rev: ATGCCAGAATCCCTCCAGAGT), *Gai3* (fwd: ATG GGACGGCTAAAGATTGACTT, rev: ATTGAGCTGATATTCCTGGA TCT), *GαO* (fwd: GGCATCGAATATGGTGATAAAG, rev: GTAGTA TTTGGCAGAGTCGTTGAG), and *Gαz* (fwd: ACGACCTGAAACTCT ACGAGGATA, rev: CTTGTACTCGGAAAGCAGATG). Relative Gα transcript levels were normalized to glyceraldehyde-3-phosphate dehydrogenase (GAPDH).

Opioid Alkaloids and Peptides. The κ-selective agonist U50,488 methanesulfonate (Von Voigtlander and Lewis, 1982) and the κ-selective antagonist norbinaltorphimine (nor-BNI) (Portoghese et al., 1987) were obtained from Sigma-Aldrich (St. Louis, MO). Nalfurafine was obtained from the National Institute on Drug Abuse Division of Drug Supply and Analytical Services. Enadoline was obtained from Parke-Davis Pharmaceuticals (Cambridge, UK). Salvinin A was purchased from ChromaDex Inc. (Irving, CA). The κ partial agonists (-)pentazocine hydrochloride (Archer et al., 1964), (-)cyclazocine hydrochloride (Archer et al., 1996), and nalmefene hydrochloride (Bart et al., 2005) were obtained from Dr. Mark Wentland (Rensselaer Polytechnic Institute, Troy, NY) (Wentland et al., 2009). ((±)-α-5,9-Dimethyl-2-(1-tetra-hydrofurfuryl)-2'-hydroxy-6,7-benzomorphan) hydrochloride (Mr 2033) was obtained from Boehringer Ingelheim (Germany). Naloxone and naltrexone were obtained from Dr. Mark Wentland (Rensselaer Polytechnic Institute, Troy, NY). Samidorphan was synthesized as previously described (Wentland et al., 2005). Dynorphin A (1–17) was purchased from AnaSpec, Inc. (Freemont, CA). Dynorphin A (1–13) and α-neoendorphin were purchased from Bachem (Torrance, CA). Dynorphin B (1–13) was purchased from GenScript (Piscataway, NJ).

Results

Using BRET Sensors to Study KOR Signaling. Since the focus of this study was to measure Gα subunit-specific activation of the KOR, we did not want to impede the KOR•Gα interaction by modifying either protein. Instead, correlating KOR activation to the release of free Gβγ was favored, similar to previous strategies (Donthamsetti et al., 2015; Masuho et al., 2015a,b). Since Gβγ functions as an obligate dimer, the BRET acceptor, Venus, was split with Venus 1–155 fused to Gγ2 or Gγ7 and Venus 156–239 fused to Gβ1 (Fig. 1). This ensured only a functional Venus (1–239) formed after Gβγ dimerization. Gβ1γ2-Venus was used for all experiments unless otherwise specified. The BRET donor, nLuc, was fused to the C-terminal end of a truncated form of the Gβγ's downstream effector, G protein-coupled receptor kinase 3 (GRK3). The C-terminal domain of this protein only contains the pleckstrin homology domain, which is responsible for Gβγ binding (Lodowski et al., 2003); the central protein kinase domain has been removed. Consequently, increased receptor phosphorylation and subsequent desensitization did not influence KOR activation. Lastly, a mas sequence (MGSSKSKTSNS) precedes the GRK3ct construct, ensuring its localization to the plasma membrane. When activation of the KOR occurred, Gα was released from Gβγ. The free Gβγ-Venus coupled with its downstream effector, masGRK3ct-nLuc, allowing for nonradiative energy transfer between nLuc and Venus and for a BRET signal to be calculated (Fig. 1).

Although BRET sensors have been used to monitor protein-protein interactions, proper controls are essential for Gα-specific data interpretation. The maximum possible BRET signal was obtained when no exogenous Gα subunit was expressed, allowing the expressed Gβ1γ2-Venus to couple to masGRK3ct-nLuc (Fig. 2A). Upon addition of 10 µM U50,488, there was no increase in the BRET ratio above baseline, signifying that endogenous Gα proteins did not affect KOR-mediated BRET signaling through an exogenously expressed Gα subunit. When Gα was expressed in excess, it served as a sink for the Gβγ and thus pulled free Gβγ away from GRK3 (Hollins et al., 2009; Donthamsetti et al., 2015). This allowed for a minimum BRET signal to be obtained (Fig. 2B). Thus, by capitalizing on the relative affinities of Gβγ to masGRK3ct-nLuc and Gα, the dynamic range of the system was determined. When the KOR, Gα subunit of interest, Gβ1γ2-Venus, and masGRK3ct-nLuc were all expressed, efficient coupling was observed as indicated by the low baseline BRET ratio (Fig. 2, C and E). Application of the κ-selective agonist, U50,488, increased the BRET ratio signifying activation; however, the stimulated ratio was well within the dynamic range of the system. Moreover, application of a κ-selective antagonist, nor-BNI, did not result in a significant increase in the BRET ratio (Fig. 2C). Lastly, to ensure the BRET ratio was a result of KOR•Gα of interest coupling, a Gα subunit from another class, Gαs, was overexpressed into the system. Again, a low baseline BRET ratio was obtained, signifying the Gβγ coupled to Gαs. Upon KOR activation with agonist U50,488, the BRET ratio remained unchanged, implying that KOR•Gαs coupling was not capable of signaling (Fig. 2D). The baseline BRET ratios across all experiments performed among the six different Gα subunits were not statistically different from each other ($P \geq 0.2$, Fig. 2E). Similarly, the maximum U50,488-stimulated ratios were

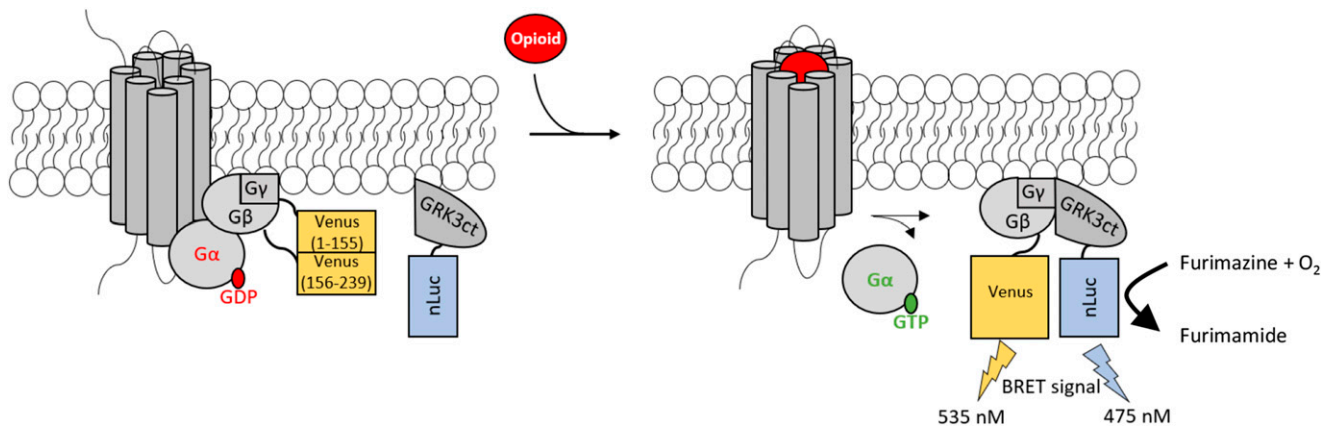


Fig. 1. Overview of the BRET assay to measure KOR signaling through different $G\alpha$ subunits. The KOR in its resting state is coupled with $G\alpha\bullet$ GDP and $G\beta\gamma$. Venus is split between $G\beta$ and $G\gamma$; thus, a fully functional Venus forms only when $G\beta\gamma$ comes together as an obligate dimer. masGRK3ct-nLuc is tethered to the membrane in the resting state. When an opioid binds to the KOR, GDP is released from the expressed $G\alpha$ subunit, and GTP binds. This binding causes dissociation of the $G\alpha\beta\gamma$ heterotrimer. $G\beta\gamma$ will then interact with its downstream target, masGRK3ct-nLuc, thus bringing nLuc and Venus in close proximity to each other. When furimazine, the substrate for nLuc, is added, nonradiative energy transfer occurs between nLuc and Venus. The BRET signal is calculated as emission of Venus at 535 nm divided by the emission of nLuc at 475 nm, which correlates to activation of the KOR through the specific $G\alpha$ subunit of interest.

not statistically different among $G\alpha$ subunits ($P \geq 0.2$, Fig. 2E).

In the experimental system, the $G\alpha$ subunit of interest was expressed in excess to minimize baseline $G\beta\gamma$ interacting with masGRK3ct-nLuc and ensure that the generated BRET signal was the result of desired $G\alpha$ subunit coupling rather than endogenous $G\alpha$. To confirm expression of the $G\alpha$ subunit in excess, Western blot analysis was performed against the individual $G\alpha$ subunits, $G\alpha_i$, $G\alpha_o$, and $G\alpha_z$ (Fig. 3A). Although expression levels using different antibodies cannot be directly compared, the $G\alpha$ subunits were expressed in excess compared with endogenous $G\alpha$ proteins (Fig. 3A). Representative curves of raw BRET ratios for U50,488 when the KOR was signaling through either $G\alpha_i1$ or $G\alpha_z$ are shown in Figure 3B. To control for subtle variation in expression level, a natural byproduct of transient transfections, all subsequent BRET data were normalized to the maximal BRET signal obtained with 10 μ M of the full agonist, U50,488. To ensure 10 μ M U50,488 produced a maximal BRET signal independent of the $G\alpha$ subunit, concentration-response curves were generated illustrating the KOR signaling through each $G\alpha$ subunit (Fig. 3C). Regardless of which $G\alpha$ subunit the KOR coupled to, the efficacy of U50,488 did not significantly vary (Fig. 3C). The EC_{50} values ranged from 1.5 ± 0.85 nM through $G\alpha_z$ to 7.9 ± 3.3 nM through $G\alpha_i2$ (Fig. 3C). In contrast to previous studies (Masuho et al., 2015b), nonsaturating concentrations of opioids were tested. A time course was generated for KOR activation to ensure adequate time for ligand-receptor interaction to reach equilibrium (Fig. 3, D and E). The BRET signal remained constant for a given U50,488 concentration when the KOR signaled through $G\alpha_i1$ regardless of time (Fig. 3D). In contrast, when the KOR signaled through $G\alpha_z$, a maximum BRET signal was obtained after 5 minutes and remained constant until the signal diminished at 120 minutes (Fig. 3E). Thus, we observed that 50 minutes allowed adequate time to obtain a maximal BRET signal at nonsaturating concentrations (Fig. 3, D and E). Subsequent data were normalized to values obtained with 10 μ M U50,488 with a 50-minute incubation performed for each individual experiment.

Dynorphin Peptide Signaling. Dynorphin and its derivatives, dynorphin A (1–17), dynorphin A (1–13), dynorphin B (1–13), and α -neo-endorphin, are endogenous KOR peptides. Concentration-response curves were generated for each peptide, and the average E_{max} and EC_{50} values were determined (Table 1). The maximal efficacy was similar for each peptide regardless of which $G\alpha$ subunit was coupled to the KOR. Interestingly, each dynorphin derivative tested was most potent when the KOR was signaling through $G\alpha_z$ compared with the other $G\alpha$ subunits. For example, the EC_{50} values of dynorphin A (1–17) were 9.6 ± 2.7 and 52 ± 11 nM when the KOR was signaling through $G\alpha_z$ and $G\alpha_i2$, respectively. A similar pattern was observed with the most potent signaling through $G\alpha_z$ for the truncated dynorphin A (1–13), producing an EC_{50} value of 0.85 ± 0.20 nM. Again, EC_{50} values of dynorphin B (1–13) ranged from 3.7 ± 2.3 nM when the KOR was signaling through $G\alpha_z$ compared with 28 ± 14 nM when the KOR was signaling through $G\alpha_i1$. Continuing with that trend, α -neo-endorphin was most potent when the KOR signaled through $G\alpha_z$, followed by $G\alpha_i3$, $G\alpha_oA$, $G\alpha_i1$, and $G\alpha_oB$, and finally least potent through $G\alpha_i2$ (Table 1). Thus, although all of the dynorphin derivatives were efficacious regardless of which $G\alpha$ subunit the KOR was signaling through, the potencies significantly varied depending on the $G\alpha$ subunit.

Full KOR Agonist Signaling Through Different $G\alpha$ Subunits. A distinct pattern emerged with dynorphin peptide signaling; however, it was unclear if opioid alkaloids would show a $G\alpha$ subunit preference as well. To obtain initial opioid profiles, classically defined KOR full agonists, U50,488, enadoline, salvinorin A, and nalfurafine, at a saturating concentration of 10 μ M were screened for KOR signaling through different $G\alpha$ subunits (Fig. 4A). Data were normalized to separate samples containing 10 μ M U50,488. Although these data are not E_{max} values as they were not obtained from a concentration-response curve, distinct signaling patterns were observed. For example, when a full agonist bound to the KOR, a maximum response was observed regardless of which $G\alpha$ subunit the KOR was signaling through as seen with U50,488, enadoline, salvinorin A, and nalfurafine (Fig. 4A).

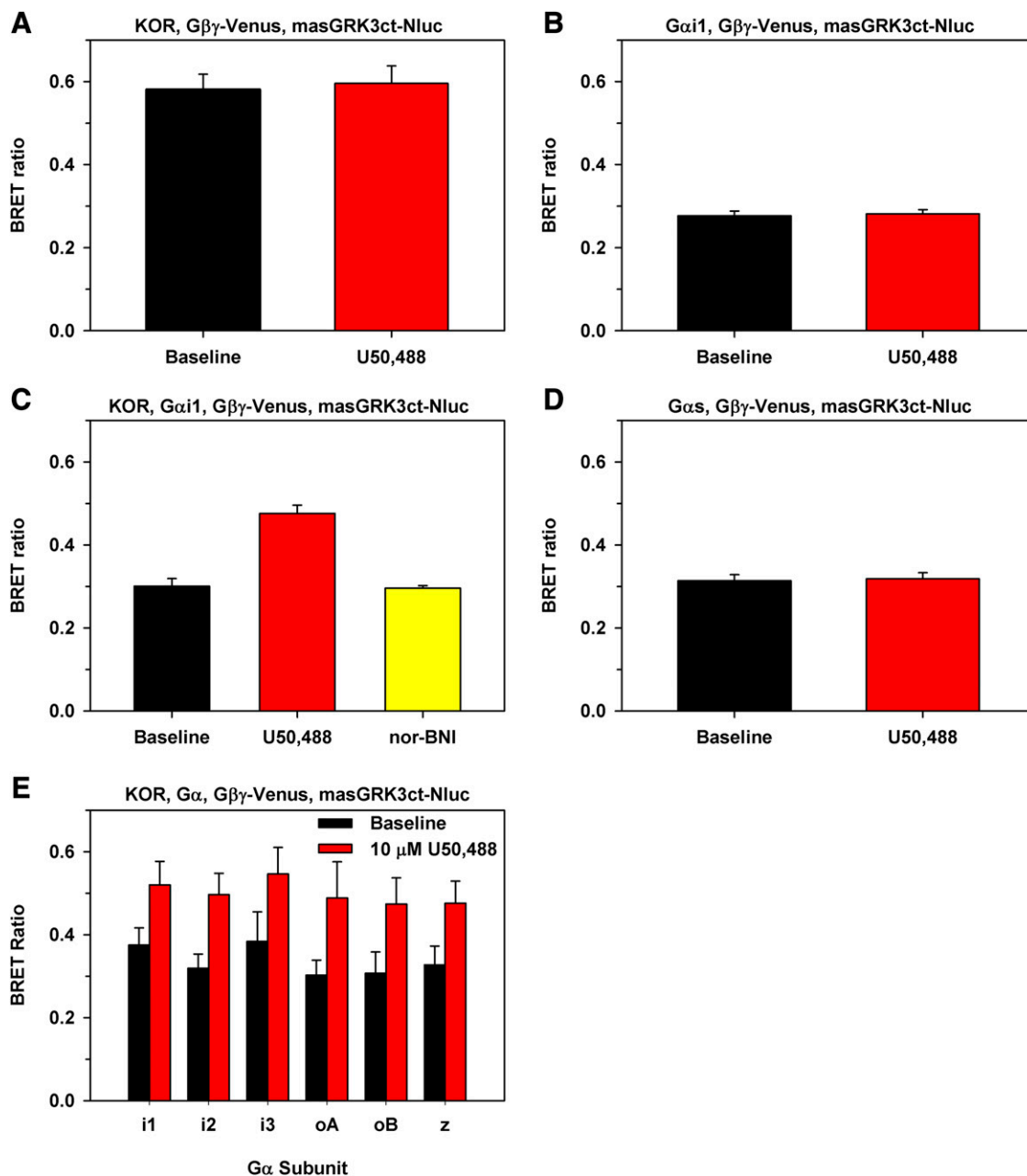


Fig. 2. BRET experimental controls. (A) The maximum BRET signal was obtained when HEK 293T cells were transfected with KOR, Gβγ-Venus, and masGRK3ct-nLuc. Since there were no exogenous Gα subunits expressed, the Gβγ-Venus couples to masGRK3ct-nLuc, and a BRET ratio of 0.58 ± 0.037 was obtained. When $10 \mu\text{M}$ U50,488 was applied, there was no change in the BRET signal, signifying that the endogenous Gα proteins did not affect the signal. (B) The minimum BRET signal was obtained when Gβγ-Venus, masGRK3ct-nLuc, and a Gα subunit of interest were expressed. In this scenario, Gβγ-Venus coupled to the Gα subunit. Since HEK 293T cells did not endogenously express the KOR, when U50,488 was applied, there was no change from the baseline BRET signal. (C) Optimal assay conditions were obtained when KOR, Gβγ-Venus, masGRK3ct-nLuc, and Gα were expressed. In the baseline condition, Gβγ-Venus coupled to Gα, and thus there was a minimal BRET signal. When the agonist U50,488 was applied, the BRET ratio significantly increased ($P = 0.003$). Lastly, when the KOR antagonist nor-BNI was applied, the BRET ratio did not change from the baseline condition ($P = 0.8$). (D) Since KOR couples to the Gαi/o class of proteins, when Gαs was expressed with KOR, Gβγ-Venus, and masGRK3ct-nLuc, no signal was transmitted when $10 \mu\text{M}$ U50,488 was applied. Data are the mean BRET ratio from three independent experiments performed in duplicate \pm S.D. (E) Baseline and U50,488-stimulated ratios for all experiments performed across the various Gα subunits. No statistically significant differences were observed between baseline and $10 \mu\text{M}$ U50,488-stimulated ratios between the Gα subunits. Data are mean BRET ratios \pm S.D.

This finding agreed with the results obtained for the dynorphin peptides (Table 1). Additionally, concentration-response curves were generated for the full KOR agonists, U50,488, salvinorin A, and nalfurafine for each Gα subunit (Table 2). Similar to the opioid peptides, salvinorin A had a similar efficacy regardless of which Gα subunit the KOR was signaling through

(Table 2). However, salvinorin A was significantly more potent when the KOR was signaling through Gαz compared with any other Gα subunit. For clarity, concentration-response curves are shown for Gαi1 and Gαz resulting in EC₅₀ values of 3.2 ± 0.83 nM and 0.36 ± 0.048 , respectively (Fig. 4B, $P = 0.0040$). Representative concentration-response curves are shown for

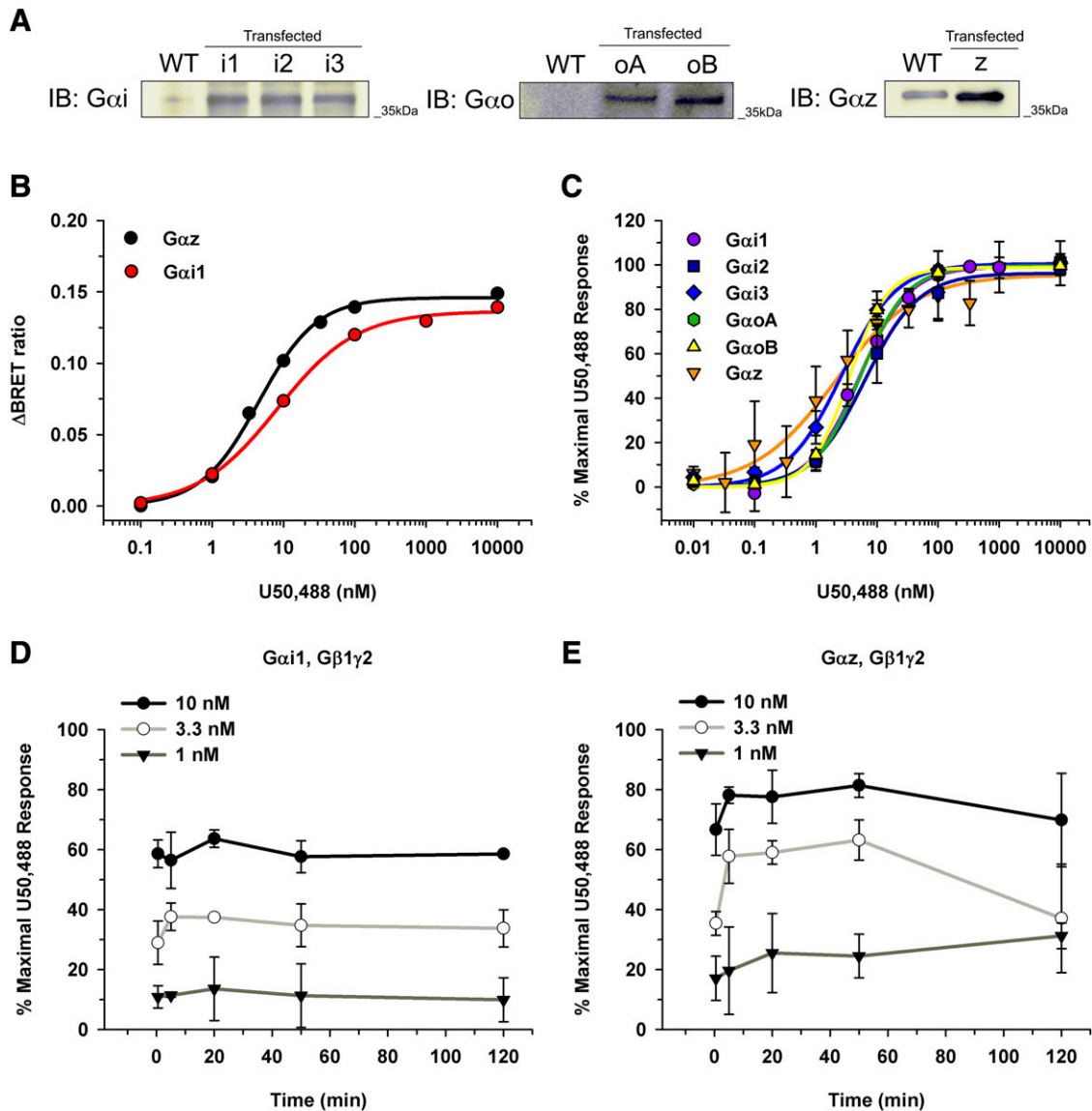


Fig. 3. Gα subunit expression level and U50,488 concentration-response and time-course experiments in HEK 293T cells. (A) To confirm overexpression of Gα subunits, Western blot analysis was performed on the individual Gα subunit transfections. Overexpression levels of Gαi1 (i1), Gαi2 (i2), Gαi3 (i3), GαoA (oA), GαoB (oB), and Gαz (z) were compared with the endogenous Gα levels in HEK 293T cells. Notably, HEK 293T cells did not express Gαo. (B) Representative concentration-response curves for U50,488 are shown illustrating raw BRET ratios for KOR•Gαz and KOR•Gαi1 after a 50-minute incubation. Ratios were calculated by subtracting opioid-induced BRET ratio from the baseline (no opioid) condition. (C) To control for variations in expression level, the BRET ratio from each experiment was normalized to 10 μM U50,488. Regardless of which Gα subunit the KOR was signaling through, U50,488 had similar E_{max} and EC₅₀ values. (D and E) Time-course experiments with varying concentrations of U50,488 were performed for the KOR signaling through Gαi1 (D) and Gαz (E). Data are from three to six independent experiments performed in duplicate with mean values ± S.D. reported. IB, immunoblot; WT, wild type.

nalfurafine signaling through Gαi1 and Gαz (Fig. 4C). Nalfurafine was maximally efficacious regardless of which Gα subunit the KOR was signaling through (E_{max} values ranging from 95% ± 2.9% through GαoB to 110% ± 8.2% through Gαz). Again, nalfurafine was significantly more potent when KOR was signaling through Gαz compared with all other Gα subunits. Nevertheless, nalfurafine had EC₅₀ values of less than 1 nM regardless of which Gα subunits were coupled to the KOR.

Partial KOR Agonist Signaling Through Different Gα Subunits. The benzomorphan partial agonists, (-)-pentazocine, (-)-cyclazocine, and Mr 2033, were also profiled at 10 μM (Fig. 5A). In contrast to full agonists, when a classically defined partial agonist bound to the KOR, the greatest activation was observed when the KOR signaled through

Gαz compared with other Gα subunits (Fig. 5A). To ensure that the 50-minute time point allowed for equilibrium to be reached without confounding any results, a time course was performed for (-)-pentazocine when the KOR was signaling through Gαi1 and Gαz (Fig. 5, B and C). Of note, the response obtained was not dependent on the incubation time. Concentration-response curves were then generated for (-)-pentazocine signaling through Gαz and Gαi1 (Fig. 5D). The E_{max} value was greater when the KOR signaled through Gαz than Gαi1 (79% ± 6.4% vs. 35% ± 9.2%, respectively). Again, a leftward shift in the curve was observed when the KOR was signaling through Gαz compared with Gαi1 (Fig. 5D) with corresponding EC₅₀ values of 7.3 ± 2.8 and 110 ± 17 nM, respectively, for (-)-pentazocine. To investigate whether the

TABLE 1

Potency and efficacy of dynorphin peptides signaling through the KOR and different $G\alpha$ subunits

Concentration-response curves were generated for the dynorphin peptides signaling through the KOR and various $G\alpha$ subunits after 50-minute incubation. Although the E_{\max} values for dynorphin A (1–17) were not significantly different regardless of the $G\alpha$ subunit ($P > 0.5$), dynorphin A (1–17) had a statistically significant lower EC_{50} value when the KOR was signaling through $G\alpha_z$ compared with the other $G\alpha$ subunits ($P \leq 0.05$). Dynorphin A (1–13) was significantly more potent when the KOR signaled through $G\alpha_z$ compared with $G\alpha_i3$ ($P = 0.011$). In addition, dynorphin A (1–13) was more efficacious through $G\alpha_z$ compared with either $G\alpha_oA$ ($P < 0.001$) or $G\alpha_oB$ ($P < 0.05$). Similarly, dynorphin B (1–13) was more potent when the KOR signaled through $G\alpha_z$ compared with $G\alpha_i1$ ($P < 0.01$). Dynorphin B (1–13) was more efficacious through $G\alpha_z$ compared than $G\alpha_oA$ ($P = 0.01$). Although α -neo-endorphin had a similar efficacy regardless of $G\alpha$ subunit ($P > 0.26$), it was significantly more potent when the KOR signaled through $G\alpha_z$ compared with all other $G\alpha$ subunits ($P < 0.05$). All values are means \pm S.D.; measurements were performed in duplicate in three independent experiments.

$G\alpha$	Dynorphin A (1–17)		Dynorphin A (1–13)		Dynorphin B (1–13)		α -Neo-Endorphin	
	EC_{50}	E_{\max}	EC_{50}	E_{\max}	EC_{50}	E_{\max}	EC_{50}	E_{\max}
	nM	%	nM	%	nM	%	nM	%
$G\alpha_i1$	23 ± 4.4	97 ± 5.0	5.8 ± 1.7	95 ± 7.0	28 ± 14	97 ± 3.1	54 ± 9.8	100 ± 5.2
$G\alpha_i2$	52 ± 11	98 ± 3.1	6.1 ± 0.45	97 ± 1.4	6.2 ± 0.50	94 ± 4.2	110 ± 40	98 ± 13
$G\alpha_i3$	45 ± 0.93	99 ± 0.97	12 ± 7.1	96 ± 6.6	13 ± 5.5	100 ± 7.5	26 ± 9.4	100 ± 6.0
$G\alpha_oA$	30 ± 8.5	91 ± 5.5	5.8 ± 0.17	70 ± 6.6	5.7 ± 1.8	88 ± 2.7	45 ± 2.3	88 ± 5.5
$G\alpha_oB$	43 ± 7.7	97 ± 11	5.9 ± 2.7	84 ± 6.5	11 ± 2.3	92 ± 1.4	78 ± 9.5	91 ± 8.8
$G\alpha_z$	9.6 ± 2.7	97 ± 6.8	0.85 ± 0.20	96 ± 3.3	3.7 ± 2.3	96 ± 6.1	6.0 ± 1.5	96 ± 4.5

$G\gamma$ subunit also affected the signaling, concentration-response curves were generated using $G\beta_1\gamma_7$. EC_{50} values of 85 ± 16 and 5.9 ± 3.5 nM were obtained when (-)pentazocine signaling through the KOR activated $G\alpha_i1$ and $G\alpha_z$, respectively (Fig. 5D). Of note, the EC_{50} values when (-)pentazocine was signaling through $G\alpha_i1 \cdot G\beta_1\gamma_7$ or $G\alpha_i1 \cdot G\beta_1\gamma_2$ were not significantly different (85 ± 16 nM vs. 110 ± 17 nM, respectively; $P = 0.14$). Similarly, EC_{50} values of (-)pentazocine were not significantly

different when the KOR coupled with $G\alpha_z \cdot G\beta_1\gamma_7$ or $G\alpha_z \cdot G\beta_1\gamma_2$ (5.9 ± 3.5 nM vs. 7.3 ± 2.8 nM, respectively; $P = 0.56$).

Concentration-response curves were generated for Mr 2033 signaling through the various $G\alpha$ subunits. EC_{50} and E_{\max} values were calculated (Fig. 5E; Table 3). Mr 2033 behaved as an efficacious partial agonist with a mean E_{\max} value of $81\% \pm 3.2\%$ when the KOR was signaling through $G\alpha_i1$. In contrast, when the KOR was signaling through $G\alpha_oB$ or $G\alpha_z$, Mr 2033

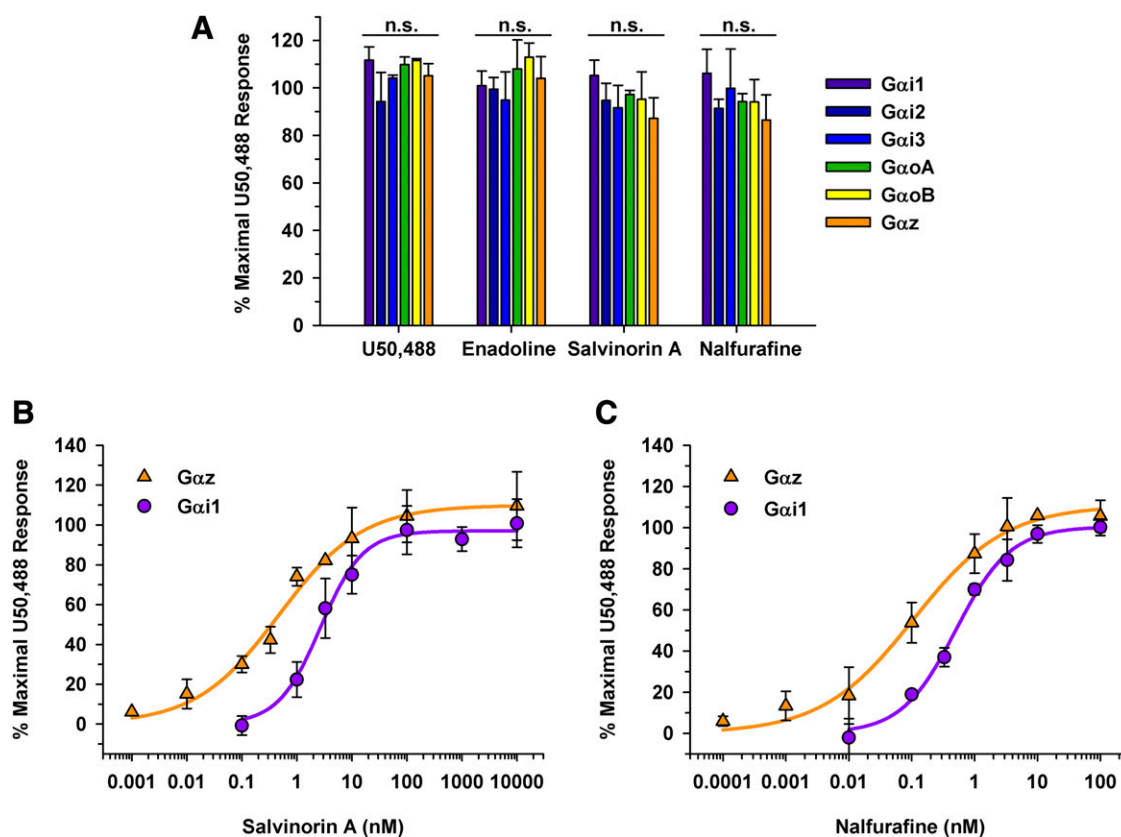


Fig. 4. KOR full agonists signaling through the KOR and different $G\alpha$ subunits. (A) Opioids were tested at a $10 \mu\text{M}$ final concentration with a 50-minute incubation in HEK 293T cells transiently expressing the KOR, $G\alpha$ subunit of interest, $G\beta\gamma$ -Venus, and masGRK3ct-nLuc. No statistically significant (n.s.) differences were observed between the various $G\alpha$ subunits for U50,488, enadoline, salvinorin A, or nalfurafine. Data are mean percentages of maximal stimulation \pm S.D.; measurements were performed in duplicate in three independent experiments. (B) Concentration-response curves were generated for salvinorin A when the KOR was signaling through $G\alpha_i1$ and $G\alpha_z$. Salvinorin A was equally efficacious whether the KOR was signaling through $G\alpha_i1$ (E_{\max} values of $99\% \pm 13\%$) or $G\alpha_z$ (E_{\max} value of $100\% \pm 11\%$) ($P > 0.05$). In contrast, salvinorin A was more potent when the KOR was signaling through $G\alpha_z$ with an EC_{50} value of 0.36 ± 0.048 nM vs. 3.2 ± 0.83 nM through $G\alpha_i1$ ($P < 0.01$). (C) Nalfurafine had similar E_{\max} values of $99\% \pm 1.1\%$ and $110\% \pm 8.2\%$ through $G\alpha_i1$ and $G\alpha_z$, respectively. Nalfurafine was more potent when the KOR was signaling through $G\alpha_z$ (EC_{50} value of 0.10 ± 0.050 nM) than through $G\alpha_i1$ (EC_{50} value of 0.46 ± 0.0040 nM) ($P < 0.01$).

TABLE 2

Full opioid agonists signaling through the KOR and different Gα subunits

Concentration-response curves were generated for U50,488, salvinorin A and nalfurafine, signaling through various Gα subunits after 50-minute incubation. E_{max} values for U50,488 were not significantly different between Gα subunits (*P* = 0.53). Although EC₅₀ values varied slightly, the EC₅₀ value for U50,488 signaling through Gαz was significantly different from Gαi1, Gαi2, and GαoA (*P* < 0.05). E_{max} values for salvinorin A did not vary between Gα subunits (*P* > 0.98); however, salvinorin A was significantly more potent when the KOR signaled through Gαz compared with all other Gα subunits (*P* < 0.01). Similarly, when the KOR was coupled to Gαz, nalfurafine was more potent compared with when the KOR was coupled to any other Gα subunits (*P* < 0.05). Nalfurafine was similarly efficacious regardless of the Gα subunit (*P* > 0.05). Data are means ± S.D.; measurements were performed in duplicate in three independent experiments.

Gα	U50,488		Salvinorin A		Nalfurafine	
	EC ₅₀	E _{max}	EC ₅₀	E _{max}	EC ₅₀	E _{max}
	nM	%	nM	%	nM	%
Gαi1	5.6 ± 1.3	99 ± 1.4	3.2 ± 0.83	99 ± 13	0.46 ± 0.0040	99 ± 1.1
Gαi2	7.9 ± 3.3	99 ± 1.1	3.1 ± 0.67	98 ± 2.1	0.38 ± 0.10	99 ± 2.1
Gαi3	2.6 ± 0.54	99 ± 1.0	2.2 ± 0.61	95 ± 5.6	0.27 ± 0.050	100 ± 7.9
GαoA	5.4 ± 0.96	99 ± 0.63	1.7 ± 0.36	100 ± 8.0	0.25 ± 0.038	99 ± 2.6
GαoB	3.5 ± 0.49	99 ± 0.31	1.6 ± 0.22	97 ± 2.8	0.37 ± 0.029	95 ± 2.9
Gαz	1.5 ± 0.85	96 ± 5.6	0.36 ± 0.048	100 ± 11	0.10 ± 0.050	110 ± 8.2

behaved as a full agonist with E_{max} values of 94% ± 3.6% and 94% ± 6.8%, respectively (Table 3). Again, Mr 2033 was most potent when the KOR was signaling through Gαz compared with any other Gα subunit (Fig. 5E; Table 3). A comparison of Mr 2033 signaling through the KOR showed a leftward shift in the concentration-response curve when the KOR signaled through Gαz compared with Gαi1. The EC₅₀ value for Mr 2033 was approximately 17-fold higher when signaling through Gαi1 than Gαz (5.4 ± 2.8 nM vs. 0.31 ± 0.15 nM, respectively). Moreover, to illustrate that the variation observed was not affected by the Gγ subunit, concentration-response curves were generated using Gβ1γ7. When the KOR coupled with Gαi1•Gβ1γ2 or Gαi1•Gβ1γ7, neither the EC₅₀ values (5.4 ± 2.8 nM vs. 5.2 ± 0.79 nM, respectively) nor the E_{max} values (81% ± 3.2% vs. 89% ± 8.5%, respectively) were significantly different. Likewise, when the KOR coupled with Gαz•Gβ1γ7, Mr 2033 was similarly potent with an EC₅₀ value of 0.19 ± 0.11 nM compared with 0.31 ± 0.15 nM when the KOR coupled with Gαz•Gβ1γ2 (Fig. 5E). Again, E_{max} values were similar regardless of the Gβγ subunit (90% ± 8.2% through Gαz•Gβ1γ7 vs. 94% ± 6.8% through Gαz•Gβ1γ2). Overall, Mr 2033 was more potent when the KOR signaled through Gαz than Gαi1 regardless of the Gβγ subunit.

Mu Opioid Receptor Antagonists Signaling Through the KOR. Since mu opioid receptor (MOR) antagonists, naloxone, naltrexone, nalmefene, and samidorphan, have partial activity at the KOR (Bart et al., 2005; Bidlack et al., 2018), a 10 μM compound screen was performed (Fig. 6A). Interestingly, as seen with partial agonists, maximal KOR signaling was attained when the KOR was coupled to the Gαz subunit, resulting in stimulation greater than 26% for each MOR antagonist. In contrast, naloxone produced less than 10% stimulation when the KOR signaled through other Gα subunits within the inhibitory class besides Gαz. A previous publication using this BRET assay reported that naloxone signaled through Gαi and Gαo (Masuho et al., 2015b). However, this previous report did not normalize the data to a full agonist to account for variability in transient transfections. Figure 6A shows that 10 μM of nalmefene and samidorphan stimulated KOR activation by 17% ± 3.7% and 16% ± 5.6% when the KOR signaled through Gαi1, respectively. Similarly, when the KOR signaled through Gαi3, 10 μM nalmefene stimulated the KOR to 11% ± 4.5%. In contrast, neither opioid activated the KOR by more than 10% when

signaling through Gαi2, GαoA, or GαoB. Concentration-response curves were generated for naltrexone with the KOR coupled to Gαz and Gαi1 (Fig. 6B). Again, a leftward and upward shift in the curve was observed when KOR was signaling through Gαz compared with Gαi1 (Fig. 6B). When the KOR coupled to Gαz, naltrexone had an EC₅₀ value of 0.32 ± 0.090 nM and an E_{max} value of 61% ± 8.8%. E_{max} and EC₅₀ values could not be calculated for naltrexone signaling through KOR•Gαi1 due to the low stimulation. Gβ1γ7 had no effect on the potency or efficacy of naltrexone compared with Gβ1γ2 (Fig. 6B). The E_{max} and EC₅₀ values were not statistically different when Gγ7 was present (64% ± 13% and 0.63 ± 0.30 nM, respectively) compared with Gγ2 (61% ± 8.8% and 0.32 ± 0.090 nM, respectively). Similarly, E_{max} and EC₅₀ values could not be calculated for naltrexone signaling through KOR•Gαi1; however, the results appear consistent between the different Gγ subunits (Fig. 6B).

To demonstrate how this assay can be used to measure antagonism and partial agonism, we sought to determine how 330 nM naloxone would shift the potency of U50,488 in the presence of the different Gα subunits. When the KOR was signaling through Gαi1, the U50,488 EC₅₀ values had an approximate 23-fold shift from 5.1 ± 1.1 to 120 ± 15 nM in the presence of naloxone (Fig. 6C). This shift was expected, as naloxone had minimal activity and behaved as an antagonist when the KOR is signaling through Gαi1 (Fig. 6A). Similarly, the U50,488 concentration-response curve had a 100-fold rightward shift when the KOR was signaling through Gαz in the presence of naloxone, with an EC₅₀ value of 170 ± 45 nM compared with 1.7 ± 0.81 nM without naloxone present (Fig. 6D). In contrast, naloxone behaved as a partial agonist and not strictly as a pure antagonist when signaling through Gαz. Subsequently, the U50,488 concentration-response curve never returned to baseline, as the 330 nM naloxone activated the KOR to approximately 34% stimulation. Thus, depending on which Gα subunit the KOR was coupled to, naloxone behaved as an antagonist (Gαi1) or partial agonist (Gαz) and shifted the U50,488 curve accordingly.

Endogenous Gα mRNA Expression Levels and Cell Line Translatability. As previously discussed, many pharmacological assays are limited by the endogenous Gα proteins expressed in a given cell line. To determine if the potential expression of endogenous Gα proteins in two commonly used cell lines might influence an assay system, mRNA levels of Gαi/o/z were determined for HEK 293 and CHO cells using

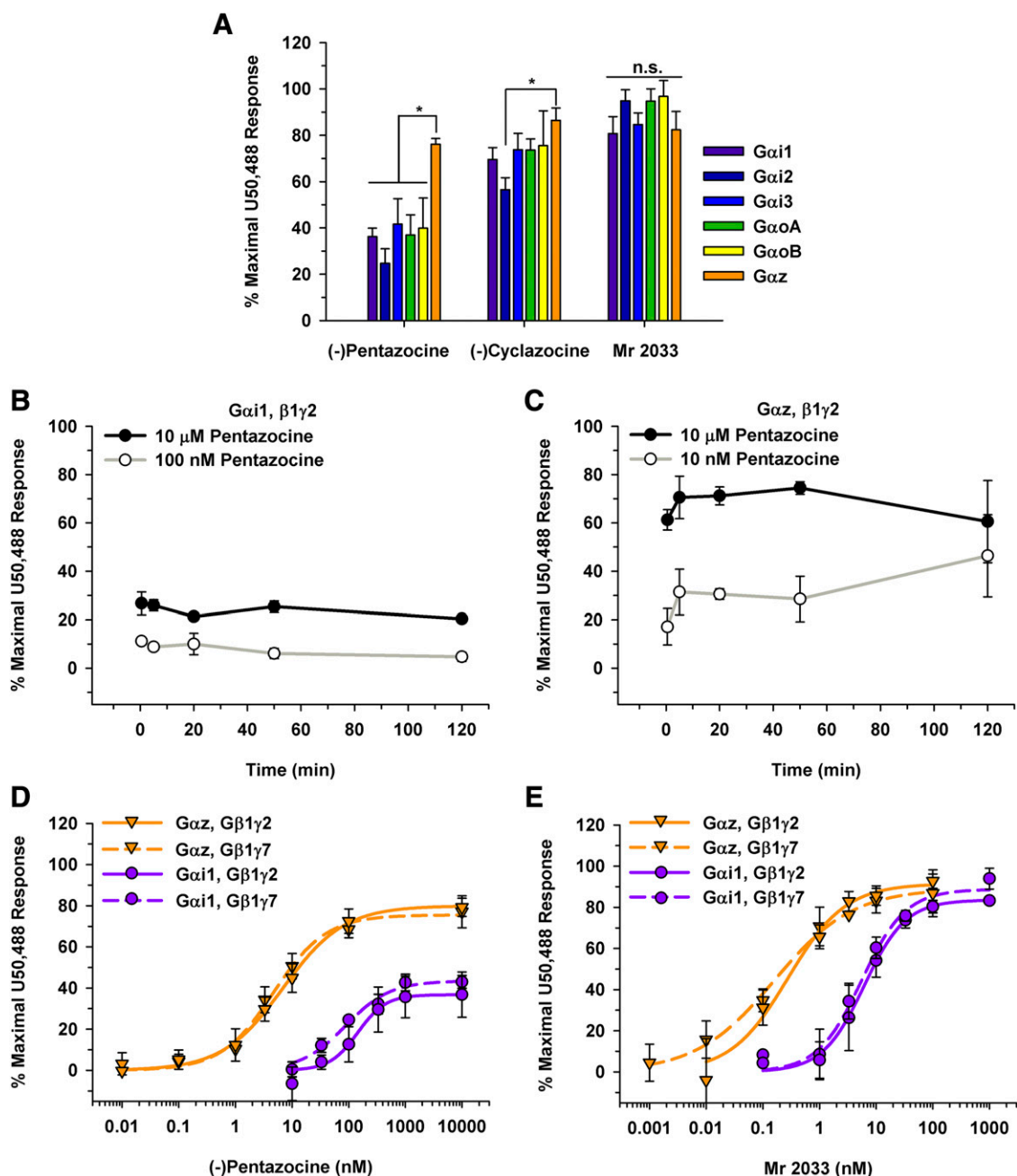


Fig. 5. KOR partial agonists signaling through the KOR and different $G\alpha$ subunits. (A) Opioids were tested at a $10\ \mu\text{M}$ final concentration with a 50-minute incubation in HEK 293T cells transiently expressing the KOR, $G\alpha$ subunit of interest, $G\beta\gamma$ -Venus, and masGRK3ct-nLuc. For (-)pentazocine, the BRET response was greatest when the KOR signaled through $G\alpha_z$ ($*P \leq 0.01$ compared with all other $G\alpha$ subunits). For (-)cyclazocine, the BRET response was significantly higher when the KOR was signaling through $G\alpha_z$ compared with $G\alpha_i2$ ($*P < 0.01$). No statistical differences (n.s.) were observed between the various $G\alpha$ subunits for Mr 2033. (B and C) Time-course experiments with (-)pentazocine were performed over a range of concentrations for $G\alpha_i1$ (B) and $G\alpha_z$ (C). No statistically significant differences were observed. (D) Concentration-response curves were generated for (-)pentazocine at the KOR signaling through $G\alpha_i1$ and $G\alpha_z$ with both $G\beta_2$ and $G\beta_7$. The EC_{50} values for (-)pentazocine of 110 ± 17 and 7.3 ± 2.8 nM signaling through $G\alpha_i1 \cdot G\beta_1\gamma_2$ and $G\alpha_z \cdot G\beta_1\gamma_2$, respectively, were statistically significant ($P = 0.010$). The E_{max} values were $79\% \pm 6.4\%$ vs. $35\% \pm 9.2\%$ signaling through $G\alpha_z$ and $G\alpha_i1$, respectively ($P = 0.002$). The EC_{50} and E_{max} values were not significantly different when the KOR was signaling through $G\beta_1\gamma_7$ compared with $G\beta_1\gamma_2$ for either $G\alpha_i1$ or $G\alpha_z$ ($P > 0.1$). (E) Mr 2033 concentration-response curves resulted in an EC_{50} value of 5.4 ± 2.8 nM when the KOR is signaling through $G\alpha_i1\gamma_2$. This value was different from the EC_{50} value of 0.31 ± 0.15 nM when signaling through $G\alpha_z\gamma_2$ ($P = 0.02$). Neither the EC_{50} value (5.2 ± 0.79 nM) nor the E_{max} value ($89\% \pm 8.5\%$) was significantly different when the KOR was signaling through $G\alpha_i1 \cdot G\beta_1\gamma_7$ compared with $G\alpha_i1 \cdot G\beta_1\gamma_2$ ($P > 0.6$). Likewise, the concentration-response curve was similar when the KOR signaled through $G\alpha_z \cdot G\beta_1\gamma_7$ compared with when the KOR signaled through $G\alpha_z \cdot G\beta_1\gamma_2$, resulting in EC_{50} values of 0.19 ± 0.11 nM and 0.31 ± 0.15 , respectively ($P = 0.3$). The E_{max} value for Mr 2033 was not different between $G\alpha_z \cdot G\beta_1\gamma_2$ and $G\alpha_z \cdot G\beta_1\gamma_7$ ($94\% \pm 6.8\%$ vs. $90\% \pm 8.2\%$, respectively; $P = 0.7$). Data are mean percentages of maximal stimulation \pm S.D.; measurements were performed in duplicate in three to six independent experiments.

TABLE 3

Potency and efficacy of the benzomorphan Mr 2033 signaling through the KOR and different Gα subunits after a 50-minute incubation

Concentration-response curves were generated for Mr 2033, signaling through various Gα subunits. Mr 2033 has similar E_{max} values, except when the KOR signaled through GαoB compared with Gαi1 ($P = 0.049$). Mr 2033 was significantly more potent when the KOR signaled through Gαz compared with Gαi1, Gαi2, Gαi3, or GαoA ($P < 0.020$). Data are means ± S.D.; measurements were performed in duplicate in three to six independent experiments.

Gα	EC ₅₀	E _{max}
	nM	%
Gαi1	5.4 ± 2.8	81 ± 3.2
Gαi2	13 ± 1.8	92 ± 5.7
Gαi3	8.0 ± 3.9	87 ± 5.0
GαoA	3.7 ± 2.1	93 ± 3.4
GαoB	6.0 ± 0.49	94 ± 3.6
Gαz	0.31 ± 0.15	94 ± 6.8

species-specific primers. Both cell lines expressed Gαi1, Gαi2, and Gαi3 (Fig. 7A); however, neither cell line expressed Gαo. Interestingly, HEK 293 cells expressed detectable levels of Gαz mRNA, which correlated with the expression of Gαz protein observed in the Western blot (Fig. 3A). In contrast, the

CHO cells did not express Gαz mRNA endogenously (Fig. 7A). Clearly, these two cell lines expressed different Gα subunits. Thus, it is feasible that performing experiments in these cell lines, which do not express Gαo, does not accurately recapitulate KOR signaling in the brain where Gαo and Gαz are expressed (Jeong and Ikeda, 1998; Jiang and Bajpayee, 2009).

Furthermore, to demonstrate the translatability of this BRET assay, key experiments were repeated in the CHO cell line. By expressing an individual Gα subunit, this assay offers the advantage of not being dependent on the endogenous Gα proteins present within a cell line. As shown in Figure 7B, U50,488 had a similar potency in CHO cells as in HEK 293T cells when the KOR was signaling through Gαi1 (EC₅₀ values of 7.3 ± 0.95 nM vs. 5.6 ± 1.3 nM, respectively) and through Gαz (EC₅₀ values of 5.0 ± 1.9 nM vs. 1.5 ± 0.85 nM vs., respectively). The partial KOR agonist (-)-pentazocine had similar efficacies in CHO and HEK 293T cells when the KOR was signaling through Gαi1 (E_{max} = 31% ± 7.0% and 35% ± 9.2%, respectively), or Gαz (E_{max} = 79% ± 6.4% and 68% ± 6.6%, respectively). Although (-)-pentazocine was slightly more potent when signaling through Gαi1 expressed in CHO cells

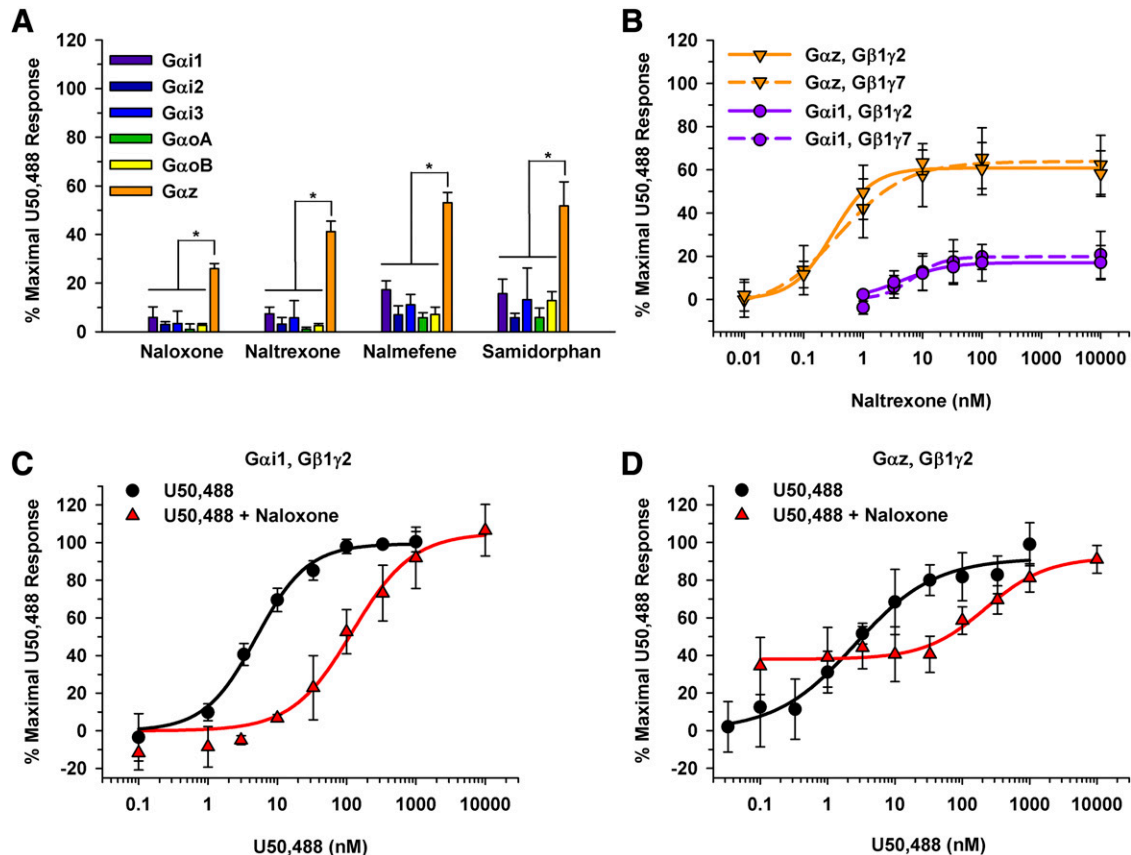


Fig. 6. MOR antagonists signaling through the KOR and different Gα subunits. (A) Opioids were tested at a 10 μM final concentration with a 50-minute incubation in HEK 293T cells transiently expressing the KOR, Gα subunit of interest, Gβγ-Venus, and masGRK3ct-nLuc. For each of the four opioids, the BRET response was greatest when the KOR signaled through Gαz (* $P \leq 0.001$ for Gαz compared with all other subunits). (B) Concentration-response curves were generated for naltrexone binding to the KOR and signaling through Gαi1 and Gαz with Gβ1γ2 or Gβ1γ7. Although E_{max} and EC₅₀ values were not calculated for Gαi1 due to low stimulation, Gβ1γ2 or Gβ1γ7 did not significantly influence the E_{max} (61% ± 8.8% vs. 64% ± 13%, respectively; $P = 0.7$) or EC₅₀ values (0.32 ± 0.090 nM vs. 0.63 ± 0.30 nM, respectively; $P = 0.1$) when the KOR was signaling through Gαz. (C and D) To demonstrate the pharmacological differences of naloxone when the KOR was signaling through Gαi1 (C) vs. Gαz (D), shifts in U50,488 concentration-response curves were observed. When the KOR was signaling through Gαi1 (C), the EC₅₀ value for U50,488 shifted from 5.1 ± 1.1 to 120 ± 15 nM in the presence of 330 nM naloxone ($P < 0.001$). Similarly, 330 nM naloxone shifted the EC₅₀ value from 1.7 ± 0.81 to 170 ± 45 nM when the KOR signaled through Gαz (D) ($P < 0.001$). The U50,488 concentration-response curve did not return to baseline and remained at approximately 34% due to naloxone acting as a partial agonist at KOR when the receptor signaled through Gαz (A). Data are mean percentages of maximal stimulation ± S.D.; measurements were performed in duplicate in three independent experiments.

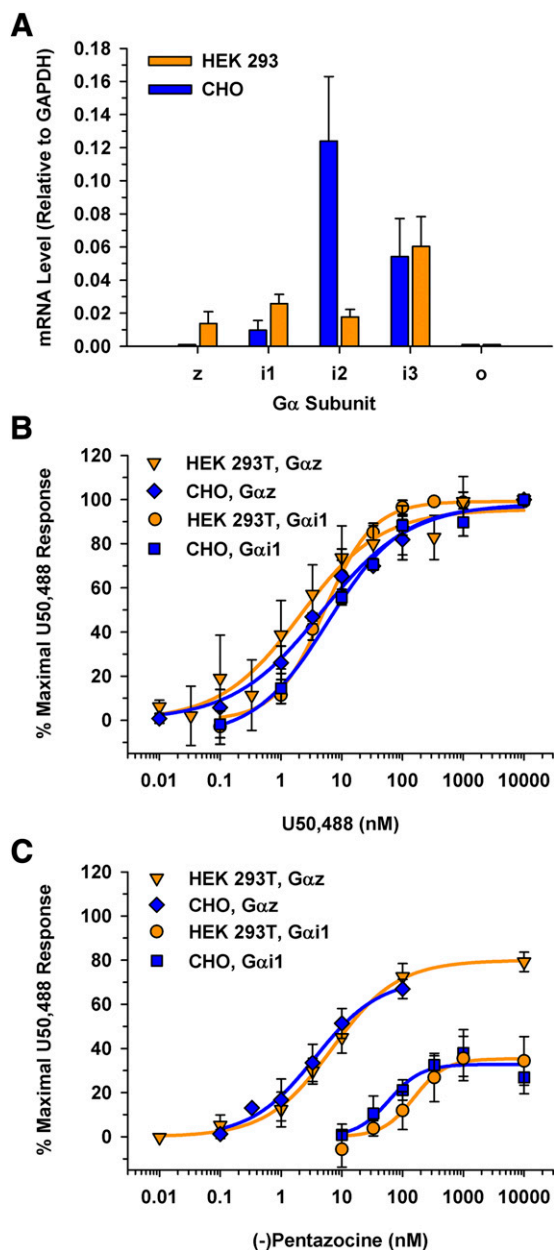


Fig. 7. Comparing mRNA levels of endogenous $G\alpha$ subunits and KOR signaling through $G\alpha_z$ and $G\alpha_{i1}$ in both HEK 293T and CHO cells as measured with BRET. (A) $G\alpha$ subunit mRNA profile in CHO and HEK 293 cells. Total mRNA was isolated from CHO and HEK 293 cell lines. Species-specific primers were used to determine relative mRNA levels to a GAPDH internal control. HEK 293 cells expressed the $G\alpha_z$ subunit transcript; CHO cells did not express detectable levels of $G\alpha_z$. $G\alpha_o$ mRNA was not detected in either cell line. Data are the mean mRNA levels relative to GAPDH from three independent experiments performed in triplicate \pm S.D. (B) U50,488 concentration-response curves were generated in HEK 293T and CHO cells after a 50-minute incubation. EC_{50} values were 7.3 ± 0.95 nM through $G\alpha_{i1}$ and 5.0 ± 1.9 nM through $G\alpha_z$ in CHO cells compared with 5.6 ± 1.3 nM through $G\alpha_{i1}$ and 1.5 ± 0.85 nM through $G\alpha_z$ in HEK 293T cells. (C) Concentration-response curves were generated for (-)pentazocine in HEK 293T and CHO cells after a 50-minute incubation. When the KOR was signaling through $G\alpha_{i1}$, an E_{max} value of $31\% \pm 7.0\%$ in CHO cells and of $35\% \pm 9.2\%$ in HEK 293T cells ($P = 0.57$). KOR• $G\alpha_{i1}$ signaling resulted in an EC_{50} value of 63 ± 24 nM in CHO cells and 110 ± 17 nM in HEK 293T cells ($P = 0.023$). (-)Pentazocine had similar E_{max} values when the KOR signaled through $G\alpha_z$ in both the CHO and HEK 293T cells (E_{max} values of $68\% \pm 6.6\%$ and $79\% \pm 6.4\%$, respectively; $P = 0.056$). (-)Pentazocine had similar EC_{50} values when the KOR signaled through $G\alpha_z$ in CHO cells (EC_{50} value of 3.3 ± 1.1 nM) and HEK 293T cells (EC_{50} value of 7.3 ± 2.8 nM) ($P = 0.051$ between cell lines).

($EC_{50} = 63 \pm 24$ nM) than in HEK 293T cells ($EC_{50} = 110 \pm 17$ nM), it was equipotent when signaling through $G\alpha_z$ in these cell lines ($EC_{50} = 7.3 \pm 2.8$ nM for HEK 293T cells and 3.3 ± 1.1 nM for CHO cells). Overall, the functional activity profiles of U50,488 and (-)pentazocine signaling through $G\alpha_{i1}$ or $G\alpha_z$ were largely unaffected by cell type.

Discussion

A BRET sensor technique was adapted to better understand $G\alpha$ -specific KOR pharmacology. By fusing the BRET donor and acceptor proteins to the $G\beta\gamma$ subunit and a truncated form of its downstream effector, GRK3, respectively, the effects of individual $G\alpha$ subunits could be observed unrestricted. In contrast to previous work (Masuho et al., 2015b), this BRET technology was used at nonsaturating opioid concentrations. By allowing the opioid and KOR to reach equilibrium, concentration-response curves were generated to calculate E_{max} and EC_{50} values. Thus, the first $G\alpha$ -specific KOR pharmacology was observed. Although no significant differences were detected between $G\alpha$ subunits when saturating concentrations of full agonists were bound to the KOR, a distinct pattern emerged when partial agonists were bound. For instance, when the KOR was signaling through $G\alpha_z$, (-)pentazocine and naltrexone had higher E_{max} values compared with KOR signaling through $G\alpha_{i1}$. Additionally, both concentration-response curves had a leftward shift when signaling through $G\alpha_z$ compared with $G\alpha_{i1}$. Since $G\beta_1\gamma_2$ is ubiquitously expressed, we sought to determine if a more striatum-specific dimer, $G\beta_1\gamma_7$ (Betty et al., 1998), would also influence KOR pharmacology. $G\gamma_2$ and $G\gamma_7$ share 66% sequence similarity (Khan et al., 2013). In contrast to the $G\alpha$ subunit, no differences in efficacy or potency were observed between $G\gamma_2$ and $G\gamma_7$ for (-)pentazocine, Mr 2033, and naltrexone. To demonstrate the utility of this assay, it was performed in both HEK 293T and CHO cell lines and resulted in similar findings. Most notably, all opioids tested were more potent when the KOR was signaling through $G\alpha_z$ regardless of cell line.

Traditional assays used to study OR signaling, such as [35 S]GTP γ S binding and cAMP levels after AC inhibition, often do not account for simultaneous signaling through various $G\alpha$ subunits (Strange, 2010). Although these assays offer some insight into OR pharmacology, it is difficult to recapitulate the complexity of signaling due to cell line limitations, namely, the differential expression of specific $G\alpha$ subunits and regulator of G protein signaling (RGS) proteins in a given cell line (Strange, 2010). For example, we determined that the relative expression of $G\alpha$ subunits was different in two commonly used cell lines, HEK 293 and CHO. Notably, neither cell line expressed $G\alpha_o$, the most abundant $G\alpha$ subunit present in the brain (Gierschik et al., 1986). Additionally, only HEK 293 cells expressed $G\alpha_z$. The mRNA distribution of $G\alpha$ proteins within HEK 293 cells agree with previous findings (Atwood et al., 2011). Though it has been established that $G\alpha_z$ is widely expressed in the brain, particularly in regions that also express ORs, its signaling properties have been less studied than the other $G\alpha_{i/o}$ -class subunits (Fields, 1998; Glick et al., 1998). Thus, a more sensitive technique was necessary to parse out the unique signaling effects of each $G\alpha$ subunit.

This novel approach to study Gα subunit-specific pharmacology may help corroborate in vitro assays with in vivo observations, thus allowing differences in agonist activation profiles to be studied. For example, intracerebroventricular administration of Gαz siRNA in mice resulted in reduced supraspinal antinociception after MOR-specific opioid administration. In contrast to other Gαi/o knockdown mice, the Gαz knockdown mice showed an impaired response to all tested opioid agonists in the 52°C warm-water tail withdrawal test (Sánchez-Blázquez et al., 1999). Furthermore, these researchers observed that the MOR agonists morphine and DAMGO ([D-Ala², N-MePhe⁴, Gly-ol]-enkephalin) had a greater potency at the MOR in mouse periaqueductal gray slices when signaling through Gαz than Gαi2 in a [³⁵S]GTPγS assay (Garzón et al., 1997). These studies suggest a prominent role for Gαz in vivo OR signaling, particularly in the context of analgesia. Although in vitro studies typically rely on Gαi/o-mediated OR signaling to predict in vivo observations, our findings further indicate the importance of understanding OR coupling to various Gα subunits and how the Gα subunits influence opioid pharmacology.

Taken together, these data indicate the importance for further study of Gαz signaling in regard to the OR. As mentioned earlier, Gαz is a member of the Gαi/o class; however, it shares the least sequence identity with the other members (Casey et al., 1990). Although Gαi/o-class subunits have a broader expression profile, Gαz has a more limited expression and is restricted primarily to the brain (Casey et al., 1990). Thus, cells that express Gαz may have a highly specialized function. Additionally, Gαz is pertussis toxin-insensitive, as it lacks the cysteine residue at the C terminus responsible for ADP-ribosylation (Ho and Wong, 1998). Although the BRET overexpression system used in this current study allowed the effects of individual Gα subunits to be observed, further study will be important to understand these signaling effects in a more physiologic context. By capitalizing on the differences in pertussis toxin sensitivity of Gαi/o and Gαz, endogenous Gαz signaling might be viewed in a physiologic environment, such as isolated primary neurons. Moreover, Gαz has a much slower intrinsic hydrolysis rate than other Gαi/o class members (Fields, 1998), which may account for some of the observed differences. Once Gαz signaling is initiated, the signaling may persist much longer than through other Gα subunits (Garzón et al., 2005). Since no exogenous RGS proteins (Hollinger and Hepler, 2002) were expressed in the current system, Gαz's slower hydrolysis rate may be contributing to the increased signal of partial agonists. Using the same BRET technique described and additionally expressing exogenous RGS proteins, future experiments can better parse out the kinetics of Gα subunit-specific pharmacology in a more physiologic environment.

In summary, this paper demonstrated the unique pharmacological profile obtained when the KOR signals through Gαz compared with other inhibitory Gα proteins. Although we acknowledge the limitations of this overexpression system, it offers insight into the intricacies of KOR•Gα signaling.

Acknowledgments

We thank Dr. Kirill A. Martemyanov for the generous gift of the BRET sensors, Dr. David I. Yule for the use of his Flexstation 3 plate reader, Dr. Angela Glading and Harsha Swamy for their assistance with the Western blots, and Dr. Cesare Orlandi for useful discussions.

Authorship Contributions

Participated in research design: Barnett, Knapp, Bidlack.

Conducted experiments: Barnett, Knapp.

Performed data analysis: Barnett, Knapp.

Wrote or contributed to the writing of the manuscript: Barnett, Knapp, Bidlack.

References

- Archer S, Albertson NF, Harris LS, Pierson AK, and Bird JG (1964) Pentazocine. Strong analgesics and analgesic antagonists in the benzomorphan series. *J Med Chem* **7**:123–127.
- Archer S, Glick SD, and Bidlack JM (1996) Cyclazocine revisited. *Neurochem Res* **21**:1369–1373.
- Atwood BK, Lopez J, Wager-Miller J, Mackie K, and Straiker A (2011) Expression of G protein-coupled receptors and related proteins in HEK293, AtT20, BV2, and N18 cell lines as revealed by microarray analysis. *BMC Genomics* **12**:14.
- Bart G, Schluger JH, Borg L, Ho A, Bidlack JM, and Kreek MJ (2005) Nalmefene induced elevation in serum prolactin in normal human volunteers: partial kappa opioid agonist activity? *Neuropsychopharmacology* **30**:2254–2262.
- Betty M, Harnish SW, Rhodes KJ, and Cockett MI (1998) Distribution of heterotrimeric G-protein beta and gamma subunits in the rat brain. *Neuroscience* **85**:475–486.
- Bidlack JM, Knapp BI, Deaver DR, Plotnikava M, Arnelle D, Wonsey AM, Fern Toh M, Pin SS, and Namchuk MN (2018) In vitro pharmacological characterization of buprenorphine, samidorphan, and combinations being developed as an adjunctive treatment of major depressive disorder. *J Pharmacol Exp Ther* **367**:267–281.
- Bidlack JM and Parkhill AL (2004) Assay of G protein-coupled receptor activation of G proteins in native cell membranes using [³⁵S]GTP gamma S binding. *Methods Mol Biol* **237**:135–143.
- Casey PJ, Fong HK, Simon MI, and Gilman AG (1990) Gz, a guanine nucleotide-binding protein with unique biochemical properties. *J Biol Chem* **265**:2383–2390.
- DeCaprio J and Kohl TO (2019) Using Dounce homogenization to lyse cells for immunoprecipitation. *Cold Spring Harb Protoc* **2019** (7) Available from: 10.1101/pdb.prot098574.
- Donthamsetti P, Quejada JR, Javitch JA, Gurevich VV, and Lambert NA (2015) Using Bioluminescence resonance energy transfer (BRET) to characterize agonist-induced arrestin recruitment to modified and unmodified G protein-coupled receptors. *Curr Protoc Pharmacol* **70**:2.14.1-2.14.14.
- Dounce AL, Witter RF, Monty KJ, Pate S, and Cottone MA (1955) A method for isolating intact mitochondria and nuclei from the same homogenate, and the influence of mitochondrial destruction on the properties of cell nuclei. *J Biophys Biochem Cytol* **1**:139–153.
- Fields TA (1998) Identification of a GTPase activating protein specific for the heterotrimeric G protein, Gz. *Cell Signal* **10**:43–48.
- Garzón J, García-España A, and Sánchez-Blázquez P (1997) Opioids binding mu and delta receptors exhibit diverse efficacy in the activation of Gi2 and G(s/z) transducer proteins in mouse periaqueductal gray matter. *J Pharmacol Exp Ther* **281**:549–557.
- Garzón J, Rodríguez-Muñoz M, López-Fando A, and Sánchez-Blázquez P (2005) The RGS22 protein exists in a complex with mu-opioid receptors and regulates the desensitizing capacity of Gz proteins. *Neuropsychopharmacology* **30**:1632–1648.
- Gierschik P, Milligan G, Pines M, Goldsmith P, Codina J, Klee W, and Spiegel A (1986) Use of specific antibodies to quantitate the guanine nucleotide-binding protein Go in brain. *Proc Natl Acad Sci USA* **83**:2258–2262.
- Glick JL, Meigs TE, Miron A, and Casey PJ (1998) RGSZ1, a Gz-selective regulator of G protein signaling whose action is sensitive to the phosphorylation state of Gαz. *J Biol Chem* **273**:26008–26013.
- Hilger D, Masureel M, and Kobilka BK (2018) Structure and dynamics of GPCR signaling complexes. *Nat Struct Mol Biol* **25**:4–12.
- Ho MK and Wong YH (1998) Structure and function of the pertussis-toxin-insensitive Gz protein. *Biol Signals Recept* **7**:80–89.
- Hollinger S and Hepler JR (2002) Cellular regulation of RGS proteins: modulators and integrators of G protein signaling. *Pharmacol Rev* **54**:527–559.
- Hollins B, Kuravi S, Digby GJ, and Lambert NA (2009) The C-terminus of GRK3 indicates rapid dissociation of G protein heterotrimers. *Cell Signal* **21**:1015–1021.
- Jeong SW and Ikeda SR (1998) G protein alpha subunit G alpha z couples neurotransmitter receptors to ion channels in sympathetic neurons. *Neuron* **21**:1201–1212.
- Jiang M and Bajpayee NS (2009) Molecular mechanisms of go signaling. *Neurosignals* **17**:23–41.
- Karlsson JO, Ostwald K, Kåbjörn C, and Andersson M (1994) A method for protein assay in Laemmli buffer. *Anal Biochem* **219**:144–146.
- Kenakin T (2011) Functional selectivity and biased receptor signaling. *J Pharmacol Exp Ther* **336**:296–302.
- Khan SM, Sleno R, Gora S, Zylbergold P, Laverdure JP, Labbé JC, Miller GJ, and Hébert TE (2013) The expanding roles of Gβγ subunits in G protein-coupled receptor signaling and drug action. *Pharmacol Rev* **65**:545–577.
- Lodowski DT, Pitcher JA, Capel WD, Lefkowitz RJ, and Tesmer JJ (2003) Keeping G proteins at bay: a complex between G protein-coupled receptor kinase 2 and Gbetagamma. *Science* **300**:1256–1262.
- Masuh I, Martemyanov KA, and Lambert NA (2015a) Monitoring G protein activation in cells with BRET. *Methods Mol Biol* **1335**:107–113.
- Masuh I, Ostrovskaya O, Kramer GM, Jones CD, Xie K, and Martemyanov KA (2015b) Distinct profiles of functional discrimination among G proteins determine the actions of G protein-coupled receptors. *Sci Signal* **8**:ra123.
- Milligan G and Kostenis E (2006) Heterotrimeric G-proteins: a short history. *Br J Pharmacol* **147** (Suppl 1):S46–S55.

- Portoghese PS, Lipkowski AW, and Takemori AE (1987) Binaltorphimine and norbinaltorphimine, potent and selective kappa-opioid receptor antagonists. *Life Sci* **40**:1287–1292.
- Rasmussen SG, DeVree BT, Zou Y, Kruse AC, Chung KY, Kobilka TS, Thian FS, Chae PS, Pardon E, Calinski D, et al. (2011) Crystal structure of the $\beta 2$ adrenergic receptor-Gs protein complex. *Nature* **477**:549–555.
- Sadana R and Dessauer CW (2009) Physiological roles for G protein-regulated adenylyl cyclase isoforms: insights from knockout and overexpression studies. *Neurosignals* **17**:5–22.
- Sánchez-Blázquez P, Gómez-Serranillos P, and Garzón J (2001) Agonists determine the pattern of G-protein activation in mu-opioid receptor-mediated supraspinal analgesia. *Brain Res Bull* **54**:229–235.
- Sánchez-Blázquez P, Rodríguez-Díaz M, DeAntonio I, and Garzón J (1999) Endomorphin-1 and endomorphin-2 show differences in their activation of mu opioid receptor-regulated G proteins in supraspinal antinociception in mice. *J Pharmacol Exp Ther* **291**:12–18.
- Stoddart LA, Johnstone EKM, Wheal AJ, Goulding J, Robers MB, Machleidt T, Wood KV, Hill SJ, and Pflieger KDG (2015) Application of BRET to monitor ligand binding to GPCRs. *Nat Methods* **12**:661–663.
- Strange PG (2010) Use of the GTP γ S ([35 S]GTP γ S and Eu-GTP γ S) binding assay for analysis of ligand potency and efficacy at G protein-coupled receptors. *Br J Pharmacol* **161**:1238–1249.
- Syrovatkina V, Alegre KO, Dey R, and Huang XY (2016) Regulation, signaling, and physiological functions of G-proteins. *J Mol Biol* **428**:3850–3868.
- Traynor JR and Nahorski SR (1995) Modulation by mu-opioid agonists of guanosine-5'-O-(3-[35 S]thio)triphosphate binding to membranes from human neuroblastoma SH-SY5Y cells. *Mol Pharmacol* **47**:848–854.
- Von Voigtlander PF and Lewis RA (1982) U-50,488, a selective kappa opioid agonist: comparison to other reputed kappa agonists. *Prog Neuropsychopharmacol Biol Psychiatry* **6**:467–470.
- Wedegaertner PB, Wilson PT, and Bourne HR (1995) Lipid modifications of trimeric G proteins. *J Biol Chem* **270**:503–506.
- Wentland MP, Lou R, Lu Q, Bu Y, VanAlstine MA, Cohen DJ, and Bidlack JM (2009) Syntheses and opioid receptor binding properties of carboxamido-substituted opioids. *Bioorg Med Chem Lett* **19**:203–208.
- Wentland MP, Lu Q, Lou R, Bu Y, Knapp BI, and Bidlack JM (2005) Synthesis and opioid receptor binding properties of a highly potent 4-hydroxy analogue of naltrexone. *Bioorg Med Chem Lett* **15**:2107–2110.
- Yung LY, Tsim ST, and Wong YH (1995) Stimulation of cAMP accumulation by the cloned Xenopus melatonin receptor through Gi and Gz proteins. *FEBS Lett* **372**: 99–102.

Address correspondence to: Dr. Jean M. Bidlack, Department of Pharmacology and Physiology, University of Rochester, School of Medicine and Dentistry, P.O. Box 711, 601 Elmwood Avenue, Rochester, NY 14642-8711. E-mail: Jean_Bidlack@urmc.rochester.edu
